

1992

Molecular and Physiological Responses of Diatoms to Variable Levels of Irradiance and Nitrogen Availability: Growth of *Skeletonema Costatum* in Simulated Upwelling Conditions


G. Jason Smith

Richard C. Zimmerman

Old Dominion University, rzimmerm@odu.edu

Randall S. Alberte

Follow this and additional works at: https://digitalcommons.odu.edu/oeas_fac_pubs

 Part of the [Environmental Monitoring Commons](#), [Marine Biology Commons](#), and the [Oceanography Commons](#)

Repository Citation

Smith, G. Jason; Zimmerman, Richard C.; and Alberte, Randall S., "Molecular and Physiological Responses of Diatoms to Variable Levels of Irradiance and Nitrogen Availability: Growth of *Skeletonema Costatum* in Simulated Upwelling Conditions" (1992). *OEAS Faculty Publications*. 118.

https://digitalcommons.odu.edu/oeas_fac_pubs/118

Original Publication Citation

Smith, G.J., Zimmerman, R.C., & Alberte, R.S. (1992). Molecular and physiological responses of diatoms to variable levels of irradiance and nitrogen availability: Growth of *Skeletonema costatum* in simulated upwelling conditions. *Limnology and Oceanography*, 37(5), 989-1007. doi: 10.4319/lo.1992.37.5.0989

Molecular and physiological responses of diatoms to variable levels of irradiance and nitrogen availability: Growth of *Skeletonema costatum* in simulated upwelling conditions

G. Jason Smith¹, Richard C. Zimmerman, and Randall S. Alberte

Department of Molecular Genetics and Cell Biology, 1103 E. 57th Street, University of Chicago, Chicago, Illinois 60637

Abstract

Molecular mechanisms that drive metabolic acclimation to environmental shifts have been poorly characterized in phytoplankton. In this laboratory study, the response of light- and N-limited *Skeletonema costatum* cells to an increase in light and NO_3^- availability was examined. C assimilation was depressed relative to N assimilation early in enrichment, and the photosynthetic quotient ($\text{O}_2 : \text{CO}_2$) increased, consistent with the shunting of reducing equivalents from CO_2 fixation to NO_3^- reduction. The concomitant increase in dark respiration was consistent with the increased energetic demand associated with macromolecular synthesis. The accelerations of N-specific rates of NO_3^- uptake and nitrate reductase activity (NRA) over the first 24 h were comparable to observations for coastal upwelling systems. Increases in cell-specific rates of these processes, however, were confined to the first 8 h of enrichment. The abundance of 18S ribosomal ribonucleic acid (rRNA) increased immediately after the environmental shift, followed by increases in levels of NR-specific mRNA that coincided with the acceleration in NO_3^- assimilation. NRA, however, exhibited a diurnal rhythm that did not correspond to changes in NR protein abundance, suggesting that enzyme activity was also regulated by direct modulation of existing NR protein by light and NO_3^- availability.

New production in the sea is driven primarily by NO_3^- assimilation (Dugdale and Goering 1967). NO_3^- is supplied to coastal upwelling systems in periodic pulses of cold, nutrient-rich water driven to the ocean surface by wind forcing (Codispoti 1983). Although upwelling systems produce dense phytoplankton blooms under certain conditions, there is a high degree of temporal and spatial variability in the production cycle, and not all upwelling systems or events

are equally efficient in converting inorganic nutrients into phytoplankton biomass (Barlow 1982; MacIsaac et al. 1985; Dugdale and Wilkerson 1989). Although system productivity ultimately depends on the total amount of nutrient introduced and the mixing environment of the system during each event (Codispoti et al. 1982), the timing and spatial extent of bloom formation may also depend on the temporal lag in physiological acclimation of the phytoplankton population to improved growth conditions (Collos 1986; Zimmerman et al. 1987).

The coastal upwelling cycle can be depicted simplistically as a conveyor belt, where phytoplankton cells advected offshore sink out of nutrient-depleted surface layers into dark, nutrient-rich water that is transported coastally and upwelled (Wilkerson and Dugdale 1987). Associated with elevated NO_3^- and irradiance levels, rates of NO_3^- uptake increase downstream along the upwelling plume, often preceding increases in C assimilation rates associated with an increase in phytoplankton biomass (MacIsaac et al. 1985; Wilkerson and Dugdale 1987; Dugdale and Wilkerson 1989). The degree of metabolic induction and subse-

¹ Correspondence and reprint requests: Hopkins Marine Station, Oceanview Blvd., Pacific Grove, California 93950.

Acknowledgments

The technical assistance of A. DeTomaso, Y. Gao, and G. Kraemer is acknowledged. We acknowledge the gift of the nitrate reductase antiserum from W. Campbell. We thank R. Dugdale for ¹⁵N analyses, J. Watanabe, R. Phillips, D. Anderson, and the staff of the Research Department of the Monterey Bay Aquarium for CHN and dissolved nutrient analyses. R.C.Z. dedicates this study to the memory of Laura Jean Grierson. Some research facilities were provided by Hopkins Marine Station of Stanford University.

This work was supported by a contract from the Office of Naval Research and, in part, by a grant from the National Science Foundation.

quent development of phytoplankton blooms depend on the mixing environment, the supply of NO_3^- , and the initial algal biomass, which collectively lead to variable rates of NO_3^- depletion as a water mass moves offshore (Zimmerman et al. 1987; Dugdale et al. 1990).

Although some of the metabolic shifts observed in natural upwelling systems may result from shifts in species composition (Chavez et al. 1990), such successional processes might reflect variable metabolic lag responses of individual species to improved conditions, which dictate the ecological success of certain members of the community. For cells exhibiting N deficiency when exposed to the improved growth conditions, the rate of induction of NO_3^- metabolism in particular, may control the dynamics of the phytoplankton bloom.

Environmental shifts that result in improved conditions can induce a suite of molecular and physiological responses that lead to higher growth rates (shift-up, Schaecter 1968). This phenomenon has been used to examine the regulatory pathways involved in the induction of specific enzyme systems and metabolic processes such as protein synthesis (Ingraham et al. 1983). Metabolic induction is of ecological importance because it often produces significant temporal lags between the stimulus (environmental shift) and the ecologically significant response (growth) that can be affected by the nature of the environmental shift, as well as the prior metabolic status of the cell (Ingraham et al. 1983). Time lags in the response of phytoplankton to improved growth conditions have been observed in the field (MacIsaac et al. 1985) and in laboratory culture (Collos 1986). Furthermore, predictions of numerical models indicate that these lags can have significant effect on the timing and intensity of phytoplankton bloom formation (Zimmerman et al. 1987). The physiological processes responsible for the observed lags, however, are poorly understood, and alternative hypotheses have been proposed to explain the field observations (Garside 1991).

Laboratory studies of unialgal cultures subjected to N starvation suggest that the temporal response to N resupply can result

in an uncoupling between N uptake and cell division (Collos 1982) and lead to variable lags in the accumulation of cellular metabolites (Sakshaug and Holm-Hansen 1977). The response of *Chlamydomonas reinhardtii* to N resupply entails, at least, differential expression of genes encoding photosynthetic functions (Plumley and Schmidt 1989). Similar regulatory processes acting on N assimilation pathways may also underlie lags in responses of marine phytoplankton to improved growth conditions.

NO_3^- assimilation is subject to some of the most extensive environmental regulation of any metabolic pathway in photosynthetic cells. The rate-limiting enzyme involved in NO_3^- assimilation in higher plants and algae, nitrate reductase (NR, EC 1.6.6.1), has been shown to be nitrate inducible (Cove and Pateman 1969; Beevers and Hageman 1980), light activated (Packard 1973; Aparicio et al. 1976; Martinez et al. 1987), and ammonium repressible (Hipkin and Syrett 1977). Additionally, given the high energetic cost of NO_3^- and NO_2^- reduction, induction of this metabolic pathway can affect the photosynthetic performance of phytoplankton. As a result, modulation of NR gene expression and enzyme activity by environmental factors may affect the time scales of NO_3^- utilization and bloom formation in the sea.

In this study, the metabolic responses of the marine diatom *Skeletonema costatum* to increased light and nutrient availability were measured to determine whether qualitative and quantitative patterns of cellular metabolic adaptation by unialgal cultures were consistent with observations of natural phytoplankton communities, define the molecular levels of control on the induction of NO_3^- metabolism by light and NO_3^- enrichment, and characterize physiological and molecular processes that can serve as useful indices of the response of phytoplankton cells to transient environmental conditions.

Materials and methods

Culture conditions—Axenic stocks of *S. costatum* (clone SKEL, obtained from the Provasoli-Guillard Center for the Culture of Marine Phytoplankton) were maintained as batch cultures in f/2 medium (Guillard

1975) at 15°C on a 14:10 L/D cycle at an incident PPF (photosynthetic photon flux) of $30 \mu\text{mol quanta m}^{-2} \text{s}^{-1}$. A 15-liter glass carboy, containing f/2 medium supplemented with $400 \mu\text{M NO}_3^-$, was inoculated with 500 ml of late-log-phase culture yielding an initial density of $2 \times 10^5 \text{ cells ml}^{-1}$. The culture was grown to stationary phase ($3.5 \times 10^6 \text{ cells ml}^{-1}$) under a 14:10 L/D cycle at a PPF of $170 \mu\text{mol quanta m}^{-2} \text{s}^{-1}$, then diluted by 50% with fresh f/2 using NH_4^+ as the sole source of N (final concn, $20 \mu\text{M}$) to repress NO_3^- metabolism (Fig. 1, point a). The culture reached stationary phase 2 d after NH_4^+ enrichment (Fig. 1, point b) and the PPF was reduced to $3 \mu\text{mol quanta m}^{-2} \text{s}^{-1}$ with several layers of neutral density screening. After 2 d under low irradiance, the culture was again diluted with f/2 containing NO_3^- as the sole N source (final concn, $60 \mu\text{M}$). The irradiance was returned to $170 \mu\text{mol quanta m}^{-2} \text{s}^{-1}$ (Fig. 1, point c) ~ 15 min after exposure to the elevated NO_3^- concentration. This last manipulation defined the start of the simulated upwelling treatment.

Bulk properties—Samples were collected daily during the light-limited period and every 4 h after the environmental shift. Macronutrient (NO_3^- , NO_2^- , NH_4^+ , and PO_4^{3-}) concentrations were determined with a flow-injection autoanalyzer (Flow Injection Systems). Cells were removed by centrifugation ($1,000 \times g$, 10 min) and the supernatant was frozen (-20°C) until analyzed for nutrient content.

Cell density was determined from the mean of cell counts in ten hemacytometer fields. Photosynthetic pigments were assayed from duplicate aliquots of the well-mixed culture collected onto Whatman GF/C filters under vacuum (20 mm of Hg). Pigments were extracted by grinding the filters in ice-cold 90% (vol/vol) acetone. Chl *a* concentrations were determined spectrophotometrically with the equations of Jeffrey and Humphrey (1975).

Particulate organic C (POC) and N (PON) were determined with a CHN analyzer (Control Equipment XA-240) on duplicate samples collected onto precombusted GF/C filters, rinsed with sterile seawater, and dried at 60°C .

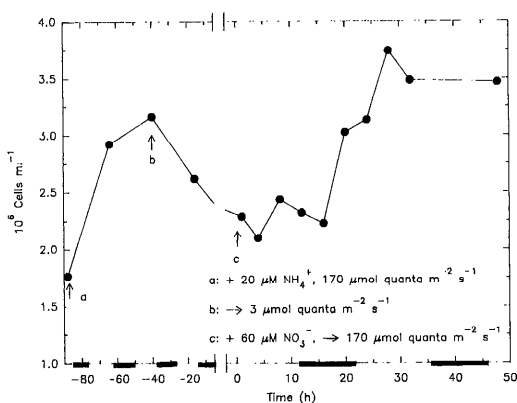


Fig. 1. Changes in *Skeletonema costatum* cell density during simulated upwelling manipulations. Point a represents time of dilution of stationary-phase, NO_3^- -grown culture with medium supplemented with NH_4^+ as sole N source. Point b represents time of low light shift-down. Point c represents time of high light and NO_3^- enrichment corresponding to the start of the simulated upwelling event or shift to improved growth conditions. Black bars indicate dark phase of 24-h light-dark cycle.

Protein and nucleic acids were quantified from duplicate samples collected onto GF/C filters, wrapped in aluminum foil, frozen in liquid nitrogen, and stored at -70°C . The frozen filters were homogenized in chilled TBS (Tris-buffered saline: 150 mM NaCl, 20 mM Tris-HCl, pH 7.5) containing 0.1% Nonidet-P40 and centrifuged. Protein content of the supernatant was determined with the bichinoic acid technique (Smith et al. 1985) with a BSA standard.

Concentrations of ribonucleic acid (RNA) and deoxyribonucleic acid (DNA) in the supernatant were determined with a fluorometric technique (Dortch et al. 1983) modified by the substitution of propidium iodide for ethidium bromide. Relative fluorescence emission was measured at $620 (\pm 5) \text{ nm}$ with $552- (\pm 5) \text{ nm}$ excitation in an Aminco SPF-500 spectrofluorometer. RNA content was determined from the difference in sample fluorescence before and after digestion with $100 \mu\text{g ml}^{-1}$ RNase A (DNase-free) for 1 h at 37°C . DNA content was calculated directly from residual fluorescence. Calf thymus DNA and torula yeast RNA were used as fluorometric standards after their concentrations had been calibrated spectrophotometrically (DNA: $1 \text{ O.D.}_{260 \text{ nm}}$

= 50 $\mu\text{g ml}^{-1}$; RNA: 1 O.D._{260 nm} = 40 $\mu\text{g ml}^{-1}$).

Physiological rate processes: Photosynthesis—Photosynthesis vs. irradiance (*P* vs. *I*) responses were measured with a polarographic oxygen electrode (Rank Brothers) kept at 15°C. Illumination was provided by a Kodak slide projector (ELH bulb). PPF was adjusted to 15 different irradiances with neutral density filters. Photosynthetic C fixation was measured on samples enriched to 1 $\mu\text{Ci ml}^{-1}$ with $\text{NaH}^{14}\text{CO}_3$ (ICN, sp act = 840 $\mu\text{Ci } \mu\text{mol}^{-1}$). Samples were incubated for 1 h in glass scintillation vials kept in a seawater-cooled (15°C) photosynthetron. Irradiance was provided by a 300-W quartz-halogen lamp and adjusted for each incubation vial with neutral-density screens. Vials wrapped with black electrical tape were used to determine dark uptake. After incubation, the contents of the vials were collected onto GF/C filters, rinsed with three volumes of sterile seawater, and acidified with 1 N HCl. Incorporation of ^{14}C was determined by scintillation counting. Quench correction used the sample channels ratio calibrated with internal standards.

Nitrate uptake— $^{15}\text{NO}_3^-$ -saturated uptake was measured at 15 different PPFs in scintillation vials incubated as described above. Each vial (20 ml) was inoculated with distilled water containing 20 mM $^{15}\text{NO}_3^-$, resulting in a 40 μM enrichment of $^{15}\text{NO}_3^-$ to the existing culture medium. Cells were collected onto precombusted GF/C filters after a 2-h incubation, rinsed with two volumes of sterile seawater, and dried at 60°C. The ^{15}N enrichment of the samples was determined with a Roboprep TracerMass mass spectrometer. $V^{15}\text{NO}_3^-$ (PON-specific $^{15}\text{NO}_3^-$ uptake rate, h^{-1}) was calculated according to Dugdale and Wilkerson (1986).

Nitrate reductase activity—Nitrate reductase activity (NRA) was measured with an in vivo assay that measured NO_2^- production by alcohol-permeabilized cells (Brunetti and Hageman 1976). For *S. costatum*, 4% (vol/vol) 1-propanol yielded the highest NRA, and the rate of NO_2^- production was linear over 2 h. Cells were collected by centrifugation (1,000 $\times g$, 5 min), resuspended in incubation medium (4% 1-propanol in sterile seawater containing 20 mM NaNO_3), and incubated in the dark at 15°C on a ro-

tary shaker table. NO_2^- concentrations were measured colorimetrically (Strickland and Parsons 1972) on aliquots (cells removed by centrifugation) taken at 15-min intervals. NRA ($\mu\text{mol NO}_2^- \text{ liter}^{-1} \text{ h}^{-1}$) was calculated from the slope of the NO_2^- concentration time series and normalized to the appropriate biomass unit.

Molecular analysis: Determination of RNA transcript abundance—Total cellular RNA was isolated with the single-step acid guanidinium isothiocyanate-phenol-chloroform method (Chomczynski and Sacchi 1987). All reagents used were molecular biology grade from Sigma. Cells were collected by centrifugation (2,000 $\times g$, 5 min, 15°C) and washed by centrifugation through sterile seawater, followed by isotonic TBS containing 5 mM EDTA at 4°C. The cell pellet was extracted with guanidinium isothiocyanate at room temperature for 1 h with intermittent vortexing. The extract was acidified with 0.1 volume of Na-acetate, pH 4.0, further disrupted by grinding in a glass homogenizer, extracted with phenol:chloroform (1:0.2, vol/vol). Aqueous and organic phases were separated by centrifugation. RNA was precipitated from the aqueous phase at -20°C after the addition of an equal volume of cold 100% isopropanol. The RNA pellet was dissolved in guanidinium isothiocyanate buffer, reprecipitated with absolute ethanol at -20°C , dissolved in diethylpyrocarbonate-treated sterile distilled water, quantified spectrophotometrically at 260 nm, and stored at -20°C as an ethanol precipitate until further analysis. RNA yield was 75–90% of the bulk RNA content determined by the fluorometric assay.

Total RNA was size fractionated by electrophoresis on denaturing 1.1% agarose-formaldehyde gels for 2.5 h at 40 V, transferred to NYTRAN membranes (Schleicher and Schuell), and immobilized by baking at 80°C under vacuum (Maniatis et al. 1982).

DNA probes were used to quantify the abundance of specific RNA transcripts. The 18S probe (DNA hybridization probe for small subunit rRNA) was generated with universal primers for small subunit rRNA (Sogin 1990) in a polymerase chain reaction (Saiki et al. 1988) amplification of *S. costatum* genomic DNA. The plasmid

pSCNR21 (DNA hybridization probe for NR transcripts) contained an 800 bp cDNA fragment isolated by screening a *S. costatum* cDNA library with a PCR (polymerase chain reaction) product synthesized with oligonucleotide primers to the NR coding sequence. The design of the NR primers was based on the amino acid sequence of the N-terminal Mo pterin and C-terminal cytochrome *b* domains of vascular plant and fungal NR (Smith and Alberte unpubl. data). Probe specificity was determined by hybridization of the northern blots with random-primed ^{32}P -labeled DNA probes with standard protocols (Feinberg and Vogelstein 1983; Wahl et al. 1987).

Temporal variation in the relative abundances of 18S and pSCNR21 homologous gene transcripts was estimated from dot blots of total RNA prepared with a BIO-DOT (BioRad) microfiltration apparatus. Equal amounts of total RNA (10 μg) from each time point were denatured with glyoxal (Thomas 1983), serially diluted with 1% SDS [sodium dodecyl sulfate (wt/vol)] before application to a NYTRAN membrane saturated with $20\times$ SSPE (1×-180 mM NaCl; 10 mM NaH_2PO_4 , pH 7.4; 1 mM EDTA), then baked and hybridized as described above. The same hybridization conditions were used for both probes: 42°C for 24 h with 2×10^6 ^{32}P cpm ml^{-1} in prehybridization-hybridization buffer [50% formamide, $5\times$ SSPE, $5\times$ Denhardt's ($1\times -0.02\%$ Ficoll 400; 0.02% BSA; 0.02% polyvinyl pyrrolidone) and 100 μg ml^{-1} sheared calf thymus DNA]. The washing conditions were: 2×15 min at 25°C in $1\times$ SSPE, 0.1% SDS; 2×15 min at 42°C in $0.1\times$ SSPE, 0.1% SDS; 3×30 min at 65°C in $0.1\times$ SSPE, 0.1% SDS.

Autoradiographs of the dot blots were analyzed on a BioImage VISAGE analytical imaging system with the Whole Band Analysis software package. Relative transcript abundances at each time point were determined from regression analysis of the integrated O.D. of each dot in the dilution series, and sequence abundance was estimated as the change in O.D. per μg total RNA.

In vitro translation—Temporal changes in the composition and abundance of translatable RNA (translational capacity) were

characterized by *in vitro* translation of 5 μg of total RNA from each sample with ^3H -leucine in a rabbit reticulocyte lysate kit (GIBCO BRL). Protein synthesis was quantified by liquid scintillation counting of 10% (wt/vol) TCA precipitates of the translation reactions and converted to dpm by the channels ratio method calibrated with internal standards. Radiolabeled translation products were separated by SDS-PAGE (Laemmli 1970) and visualized by fluorography (Bonner and Laskey 1974).

Polypeptide composition and western blotting—Changes in cellular polypeptide composition were monitored by SDS-PAGE (polyacrylamide gel electrophoresis) analysis of the same detergent extracts used for protein and nucleic acid quantifications. Subsamples of the extracts were apportioned to equivalent protein content, precipitated on ice with cold (0°C) 80% (vol/vol) acetone, and resolubilized with SDS-PAGE sample buffer (Laemmli 1970). Variation in the relative abundance of NR was determined from western blots of SDS-PAGE gels (Towbin and Gordon 1984) probed with heterologous, polyclonal antisera to squash-leaf NR (Redinbaugh and Campbell 1983). Immunoreactive polypeptides were localized on nitrocellulose blots with alkaline phosphatase-coupled, goat-antirabbit secondary antibodies. The integrated O.D. of each immunoreactive band was used directly as the index of NR abundance normalized to equivalent protein content.

Results

Cell growth during the simulated upwelling cycle—Cell numbers changed in a predictable pattern throughout the manipulation (Fig. 1). The addition of NH_4^+ 48 h before the transfer to light-limited conditions (Fig. 1, point a, -88 h) led to a single doubling in cell number. The culture was approaching stationary phase when transferred to a PPF below photosynthetic compensation (Fig. 1, point b, -40 h; see below), during which time cell density declined by 17%. The light and NO_3^- enrichment (Fig. 1, point c, 0 h) led to another round of cell division that was completed at $+30$ h. The culture returned to stationary phase after a

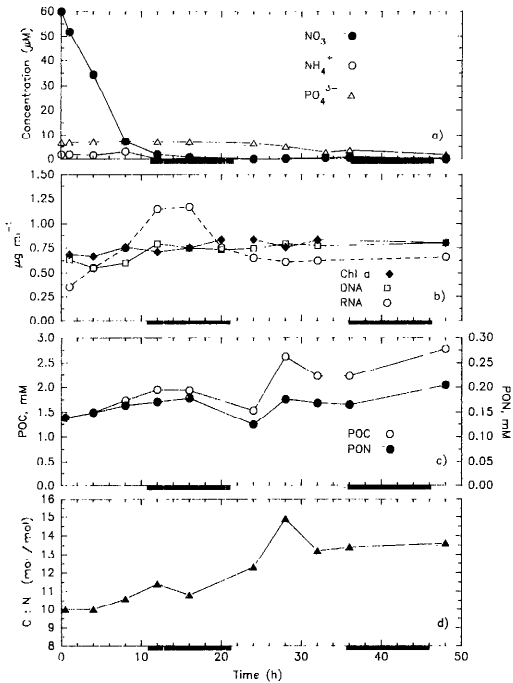


Fig. 2. Changes in dissolved nutrient concentrations and biomass indicators of the *Skeletonema costatum* culture after the shift to improved growth conditions. [a.] Dissolved NO_3^- , NH_4^+ , and PO_4^{3-} concentrations in the growth medium. [b.] Concentrations of Chl *a*, DNA, and RNA. [c.] Concentrations of POC and PON. [d.] Variation in the C:N atomic ratio in the particulate fraction.

1.7-fold increase in cell number. About 10% of the cells observed in the stationary-phase culture 48 h after enrichment were spermatogonia, but none were observed before this time.

Nutrient utilization—The NO_3^- enrichment (60 μM), relative to the standing stock of cell nitrogen was 0.43 (DIN: PON) and was depleted from the medium after 24 h (Fig. 2a). The residual NH_4^+ concentration was 2 μM at 0 h, and no net uptake of NH_4^+ occurred until the NO_3^- concentration dropped below 10 μM , ~ 10 h after enrichment. Orthophosphate remained relatively constant until 28 h after enrichment, then decreased by 60% over the next 4 h following the completion of cell division. NO_2^- concentrations remained below 1 μM throughout the experiment. The rate of NO_3^- depletion was constant [6.9 (± 1.2) μmol

$\text{NO}_3^- \text{ liter}^{-1} \text{ h}^{-1}$] over the first 8 h after enrichment.

Bulk properties—Concentrations of Chl *a*, DNA, and RNA in the culture tracked the decline in cell density during the light-limited phase (-40 to 0 h), indicating no net synthesis of these components during this period (data not shown). In contrast, the shift to improved environmental conditions resulted in a 20% increase in the volume-specific content of Chl *a* between 0 and +20 h and a 32% increase in DNA content between +8 and +12 h (Fig. 2b). Volume-specific levels of RNA exhibited a transient, 3-fold increase between 0 and +12 h, then declined over the subsequent 4 h to a level 50% above the value at 0 h. POC and PON levels also increased over the first 16 h (Fig. 2c). POC accumulated more rapidly than PON after +8 h, reflecting the onset of N depletion. POC content, however, increased an additional 40% during the second light period after enrichment (+20 to +32 h), indicating significant net photosynthesis over this interval. The C:N atomic ratio in the particulate fraction increased from 10.5 at +8 h to 13 at +30 h after enrichment (Fig. 2d), reflecting the rapid depletion of NO_3^- from the medium and indicating that the NO_3^- pulse was not sufficient to overcome the N deficiency exhibited by the cells at the end of the light-limited phase.

Metabolic rate processes: NO_3^- uptake— $V^{15}\text{NO}_3^-$ accelerated at a rate of $7.4 \times 10^{-4} \text{ h}^{-2}$ between +1 and +24 h to a maximum of 0.033 (± 0.004) h^{-1} and then declined immediately after cell division (Table 1; Fig. 3a). Uptake of ^{15}N was independent of PPF during all of the 2-h incubations (data not shown) and average rates for each time point were calculated by pooling the samples measured at the 15 irradiances. Estimates of $V^{15}\text{NO}_3^-$ accounted for only 41% of the observed NO_3^- depletion rate in the culture during the first 8 h of the simulated upwelling (Table 2), possibly indicating a loss of $^{15}\text{NO}_3^-$ from cellular pools during sample drying or by DON production.

Nitrate reductase activity—VNRA (PON-specific NRA, h^{-1}), exhibited a pronounced diurnal rhythm (Fig. 3) that peaked in the middle of the light period. Average NRA

Table 1. Acceleration of N-specific $^{15}\text{NO}_3^-$ incorporation, $V^{15}\text{NO}_3$, and in vivo NRA, $V\text{NRA}$, in *Skeletonema costatum* between 0 h and +24 h of the simulated upwelling. Acceleration of $V\text{NRA}$ peak activity was determined from the difference in the peaks in NRA between the first two light periods. Based on data in Fig. 3a.

Parameter	Acceleration ($\times 10^{-4} \text{ h}^{-2}$)
$V^{15}\text{NO}_3$	7.4
$V\text{NRA}$	2.4
$V\text{NRA}$, peak activity	0.6

was equivalent to $\sim 50\%$ of the $^{15}\text{NO}_3^-$ uptake rate during the first and second light periods after enrichment (Table 2, Fig. 3a). No recovery of NRA was observed during the third light period after NO_3^- had been depleted from the medium for 24 h. As with NO_3^- uptake, maximal NRA increased between 0 and +24 h after enrichment (Table 1). Acceleration of NRA over the first 24 h was 65% of the rate for $V^{15}\text{NO}_3$, whereas the daily peak in NRA increased at only 18% of the rate observed for ^{15}N uptake. The lack of light dependence in $V^{15}\text{NO}_3$ and pronounced light-dependent phasing of $V\text{NRA}$ demonstrated that uptake and assimilation were uncoupled.

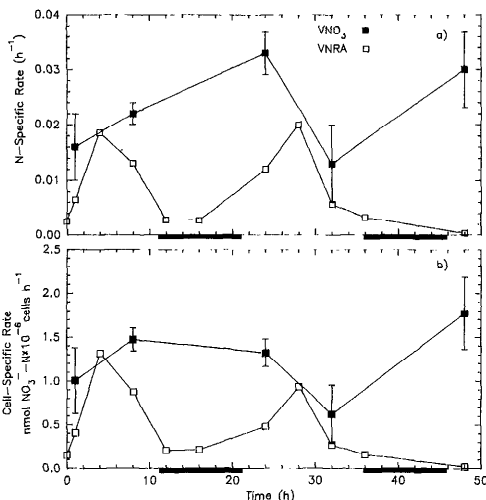


Fig. 3. Variation in $^{15}\text{NO}_3^-$ uptake capacity and in vivo NRA of *Skeletonema costatum* after shift to improved growth conditions. [a.] Rates normalized to PON content. [b.] Rates normalized to cell number.

Table 2. Comparison of mean PON-specific rates (± 1 SD) of NO_3^- depletion ($V\text{NO}_{3\text{dep}}$), NO_3^- -saturated uptake of $^{15}\text{NO}_3^-$ ($V^{15}\text{NO}_3$), and NRA ($V\text{NRA}$) in *Skeletonema costatum* between 0 and +24 h of the simulated upwelling (based on data in Figs. 2, 3a).

Parameter	Rate (h^{-1})
$V\text{NO}_{3\text{dep}}$	0.046 ± 0.011
$V^{15}\text{NO}_3$	0.019 ± 0.003
$V\text{NRA}$	0.010 ± 0.007

The patterns of induction observed for $^{15}\text{NO}_3^-$ uptake and NRA were different when standardized to cell number rather than the N content of the culture (Fig. 3b). Although N-specific and cell-specific rates of $^{15}\text{NO}_3^-$ uptake exhibited similar increases from 0 to +8 h after enrichment (37 and 47%, respectively), the cell-specific uptake capacity did not continue to increase. Similarly, cell-specific NRA values exhibited only an 18% increase from 0 to +24 h after enrichment, compared to an 85% increase in N-specific activity. Again NO_3^- uptake and assimilation were not in phase. Additionally, cell-specific NRA was lower at +28 h than at +4 h (Fig. 3b), indicating that cell-specific measures were more indicative of NO_3^- depletion from the medium.

Photosynthesis and respiration—Light compensation (I_c) and saturation (I_k) PPFs for oxygenic photosynthesis did not change after the shift to improved growth conditions, remaining above [$I_c = 7.9 (\pm 2.8) \mu\text{mol quanta m}^{-2} \text{ s}^{-1}$, $N = 4$, 0–48 h] and below [$I_k = 73.4 (\pm 18.2) \mu\text{mol quanta m}^{-2} \text{ s}^{-1}$, $N = 4$, 0–48 h] the PPFs used for the light-limited and simulated upwelling treatments, respectively. In contrast, maximal Chl *a*-specific rates of net oxygen evolution and gross carbon (^{14}C) assimilation varied dramatically (Table 3). Oxygenic photosynthesis and dark respiration increased by 23 and 78%, respectively, between 0 and +8 h, while *C* assimilation rates dropped by 43% during the same period. This pattern resulted in a 4-fold reduction in the *P*:*R* ratio (Table 3).

Associated with the increase in oxygenic photosynthesis at +8 h was a 2-fold increase in photosynthetic efficiency (α), which returned to the pre-enrichment level by +32 h. After the culture reached stationary phase

Table 3. Variation in photosynthetic efficiency (α), light-saturated photosynthetic rates of gross oxygen evolution ($P_{\max} O_2$), dark respiration (RO_2), C assimilation ($P_{\max} {}^{14}C$), photosynthetic quotients ($O_2 : CO_2$), and ratios of oxygenic photosynthesis to respiration ($P : R$) during the light and NO_3^- shift-up of *Skeletonema costatum*. Daily oxygenic $P : R$ ratios were calculated based on 14 h of light-saturated net photosynthesis and 24 h of dark respiration: $[(P_{\max} O_2 - RO_2) \times 14] / [RO_2 \times 24]$.

Time (h)	α^*	$P_{\max} O_2 \dagger$	$RO_2 \dagger$	$P_{\max} {}^{14}C \ddagger$	$O_2 : CO_2$	$P : R$	Daily $P : R$
0	3.6(1.0)	331(28)	20(5)	241(18)	1.37	16.4	9.0
8	7.8(1.6)	408(31)	93(25)	137(7)	2.98	4.4	2.0
32	3.4(0.2)	283(6)	26(5)	155(7)	1.83	11.0	5.8
48	4.3(0.4)	278(7)	28(6)	213(5)	1.31	9.8	5.2

* $[\mu\text{mol } O_2 \text{ (mg Chl } a \text{)}^{-1} \text{ h}^{-1}] [\mu\text{mol quanta } m^{-2} \text{ s}^{-1}]^{-1} (\pm 1 \text{ SD})$.

† $\mu\text{mol } O_2 \text{ (mg Chl } a \text{)}^{-1} \text{ h}^{-1} (\pm 1 \text{ SD})$.

‡ $\mu\text{mol } CO_2 \text{ (mg Chl } a \text{)}^{-1} \text{ h}^{-1} (\pm 1 \text{ SD})$.

(ca. +28 h), oxygenic photosynthesis stabilized, but rates of C assimilation increased. These shifts resulted in a more than doubling of the photosynthetic quotient ($PQ = O_2 : CO_2$) between 0 and +8 h, followed by a return to the initial PQ value after the culture reached stationary phase (Fig. 4; Table 3). Calculation of daily $P : R$ ratios indicates that, under conditions of high rates of NO_3^- assimilation (+8 h), daily photosynthetic C gain would only slightly exceed C demand (Table 3).

The ratio of C- and N-specific C : N uptake capacity was 7.7 at the onset of the simulated upwelling treatment but dropped below 5 for the remainder of the experiment (Fig. 4). If we assume that the Redfield value

of 6.6 represents balanced uptake capacity, the changes observed here indicate a large increase in the capacity to take up N relative to C immediately after the nutrient pulse. These findings are consistent with the changes in photosynthetic and respiratory energetics and are reflected in the variation in the PQ and $P : R$ ratios described above.

Molecular processes: Macromolecular pools—Cellular content of Chl *a*, DNA, RNA, and protein in *S. costatum* declined during the light-limited period (−40 to 0 h; Fig. 5a,b). The shift to improved growth conditions resulted in sequential accumulation of nucleic acids and proteins that preceded cell division. RNA content increased 3.5-fold in the first 12 h after enrichment. This accumulation of RNA, indicative of increased transcription, preceded net protein synthesis by 4 h and DNA synthesis by 8 h. Chl *a* content increased gradually (~10%) and then decreased by 28% after cell division, most likely reflecting the onset of N depletion. Cellular protein content was 66% higher after cell division whereas total nucleic acid content (RNA + DNA) decreased to pretreatment levels. The RNA content, relative to cellular DNA, increased 1 h after enrichment and declined exponentially after cell division to the pre-enrichment ratio (Fig. 5c), providing further evidence for transcriptional activation by light and NO_3^- enrichment.

Characterization of changes in the RNA transcript population: Translational capacity—The abundance of translatable RNA increased by 69% between 0 and +8 h and was associated with the initial doubling in total RNA content (Fig. 6a). Although total

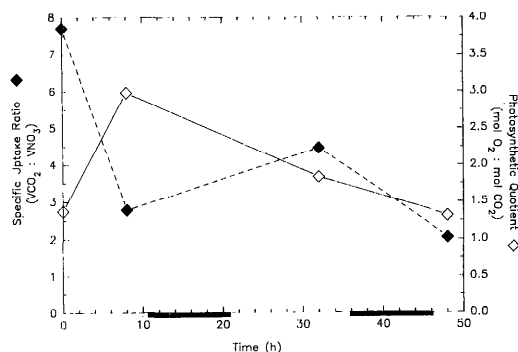


Fig. 4. Changes in photosynthetic quotient and the ratio of specific rates of C and NO_3^- uptake following light and NO_3^- enrichment of *Skeletonema costatum*. The photosynthetic quotient was computed from data in Table 3. The relative capacity for inorganic C uptake (photosynthesis) and NO_3^- uptake was calculated as the ratio of C-specific, light-saturated photosynthetic ${}^{14}C$ incorporation (VCO_2 , h^{-1}) and N-specific NO_3^- uptake capacity ($V^{15}NO_3$, h^{-1}).

RNA content continued to increase until the onset of cell division at +20 h, the abundance of translatable RNA declined, indicating that the continued increase in total RNA was associated with the accumulation of ribosomal and other nonmessenger RNAs. A second peak in translatable RNA occurred at +28 h, after the completion of cell division. Translational capacity declined subsequently as the cells entered stationary phase.

Analysis of the *in vitro* translation products by SDS-PAGE revealed that the initial response to improved growth conditions was associated with the accumulation of transcripts encoding a suite of polypeptides ranging from 20 to 40 kD (kilodaltons) between 0 and +8 h (Fig. 6b). A similar set of polypeptides was synthesized at the time of the second peak (24 h) in translatable RNA content. No measurable synthesis of polypeptides in the 100–120-kD mol wt size class expected for NR (Solomonson and Barber 1990; Y. Gao and G. J. Smith unpubl. data) was observed that corresponded to the variation in NRA however, probably attributable to the low abundance of NR relative to total cellular protein (*see below*).

Hybridization analysis of the transcript population—Northern analysis of total cellular RNA from *S. costatum* revealed that the 18S and pSCNR21 probes hybridized to discrete bands with relative lengths of 1.8 kb (kilobase) for the small subunit ribosomal transcript and 5.0 kb for the NR transcript, respectively (Fig. 7). The specificity of these probes made them amenable for quantifying temporal changes in specific transcript abundance by dot-blot analysis.

Abundance of 18S rRNA declined by a factor of 2 under light limitation (−40 to +1 h), then increased by a factor of 2.5 at +4 h (Fig. 8a,c,d). The relative abundance of 18S rRNA increased an additional 3.5-fold between +12 h and +32 h, after the completion of cell division. The two peaks in 18S rRNA abundance were associated with the periods of maximal translational capacity (*see Fig. 6a*). The first maximum in 18S rRNA abundance preceded acceleration in the rate of cellular protein accumulation and the initial increase in translational capacity (*see Figs. 5b, 6a*). The

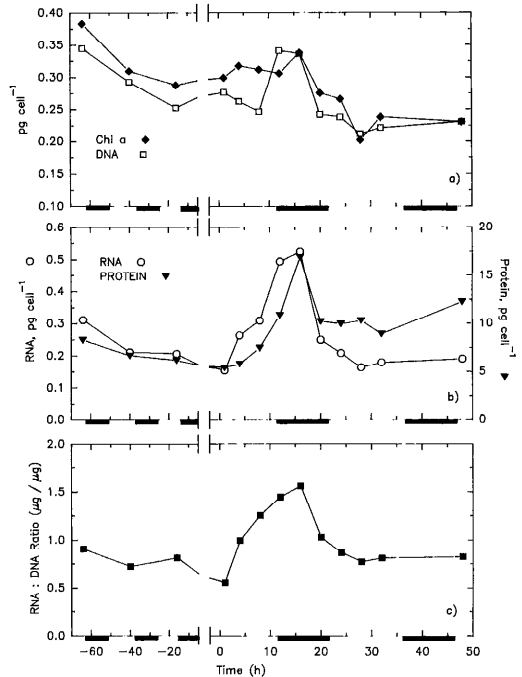


Fig. 5. Variation in cellular constituents of *Skeletonema costatum* during NO_3^- -depleted and light-limited (−60 to 0 h) growth and following light and NO_3^- enrichment. [a.] Chl *a* and DNA content. [b.] RNA and protein content; note increase in scale for RNA axis compared to panel a. [c.] Ratio of cellular RNA and DNA, indicating a pulse of transcription that may characterize the initial response to improved growth conditions. (Note change of scale in time axis after break.)

second increase in 18S rRNA abundance was greater than the first peak (Fig. 8c) and paralleled the increase in translational capacity between +12 and +24 h (Fig. 6a), although 18S rRNA abundance peaked at +32 h, 8 h after the peak in translational capacity,

The exposure slopes of the pSCNR21 probed dot blot (Fig. 8b) were 10–100-fold lower than those for the 18S probe (Fig. 8c), implying a lower abundance for the transiently expressed NR transcript. The relative abundance of the pSCNR21-positive transcript declined 80% during the light-limited period (−40 to 0 h, Fig. 8d). After the shift to improved growth conditions, NR transcript abundance increased 380% between 0 and +4 h, then declined 50% during the dark period through +16 h (Fig. 8c,d). The abundance of the NR transcript in-

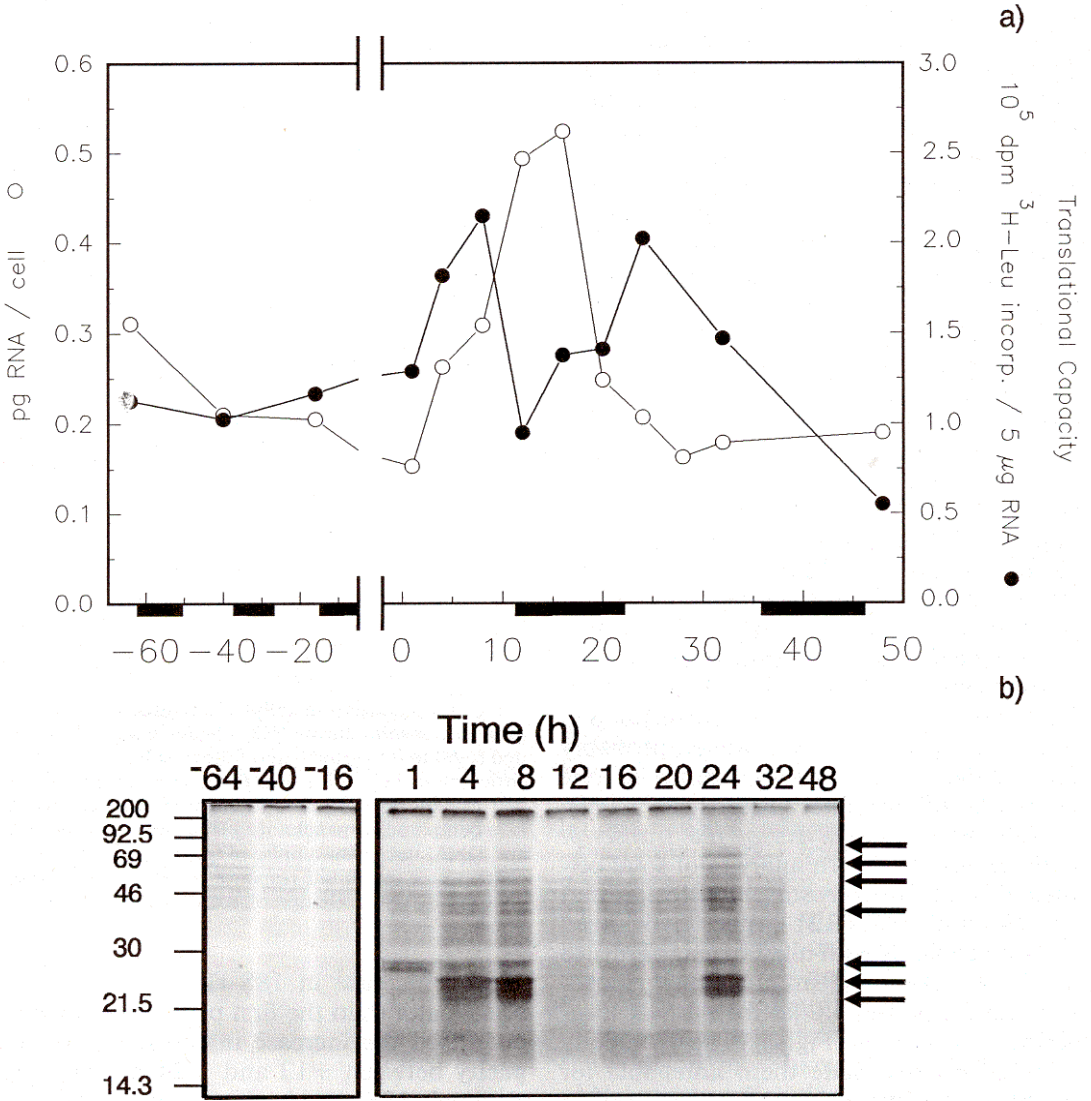


Fig. 6. Characterization of changes in translational capacity and in vitro translation products of total RNA isolated from *Skeletonema costatum* during simulated upwelling. [a.] Variation in total cellular RNA (as in Fig. 5b) and the translational capacity, the amount of protein synthesis (³H-leucine incorporation) supported by 5 μg of total RNA in an in vitro translation reaction. [b.] Autoradiograph of the in vitro translation products generated in the reactions quantified in panel a. Equal reaction volumes (5 μl), with variable amounts of labeled protein (as indicated in panel a) were loaded per lane and separated by 12.5% SDS-PAGE and visualized by fluorography. The positions of mol-wt markers (kD) indicated on the left axis. Arrows indicate position of labeled polypeptides whose abundance varied with time after enrichment.

creased gradually during the second light period, reaching a maximum at +32 h, coincident with the second peak in 18S transcript abundance. The abundance of the NR transcript declined over the next dark period to pre-enrichment levels at +48 h, as

the culture was in stationary phase in the NO₃⁻-depleted medium.

Regulation of NRA—The NR protein was detectable in profiles of *S. costatum* protein only by immunological methods. Western blots of total proteins probed with a het-

erologous polyclonal NR antiserum revealed an immunoreactive polypeptide in the molecular size range (105–110 kD) observed for higher plant (Solomonson and Barber 1990) and purified *S. costatum* NR (Y. Gao and G. J. Smith unpubl. data; Fig. 9a). Protein-specific abundance of this polypeptide declined by a factor of 3 during the light-limited phase (–40 to 0 h), increased by a factor of 1.5 in the first hour after enrichment, then declined by a factor of 2 at +8 h (Fig. 9b). Abundance of the NR polypeptide increased by a factor of 3.3 during the dark period prior to the onset of cell division (+8 to +12 h), then declined at the beginning of the second light period after enrichment (+20 to +28 h). NR protein level increased again from +28 to +48 h after enrichment.

Comparison of variation in NRA with NR polypeptide and transcript abundance provides insight into the levels of regulation controlling NRA during transition to improved growth conditions. The cellular content of NR protein and transcripts declined by 80% during the light-limited period, then increased by 30% in the first hour after the light and NO_3^- enrichment (Fig. 10). The dramatic increase in NR transcript abundance between 0 and +4 h preceded a similar increase in NR protein through the first half of the dark period between +8 and +16 h. This pattern was observed again between +22 and +48 h after enrichment, but increases were of lower magnitude. Although accumulation of NR transcripts during the light period was correlated with peaks in NRA, the lack of a concomitant increase in NR protein suggests that the diurnal rhythm in NRA resulted from the light activation of existing NR protein.

When expressed as relative levels per cell (Fig. 10), in vivo NRA increased by 280% between 0 and +4 h, although no similar increase in the cellular content of NR protein was observed. The subsequent decline in NRA (37%) between +4 and +8 h was associated with a decline (20%) in NR protein abundance. The low NRA observed during the first dark period, however, was associated with a dramatic increase in NR protein abundance. Cellular NR protein

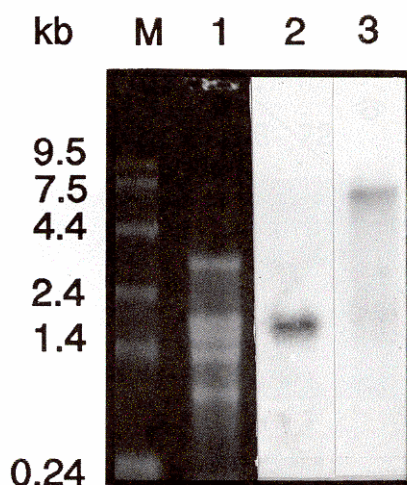
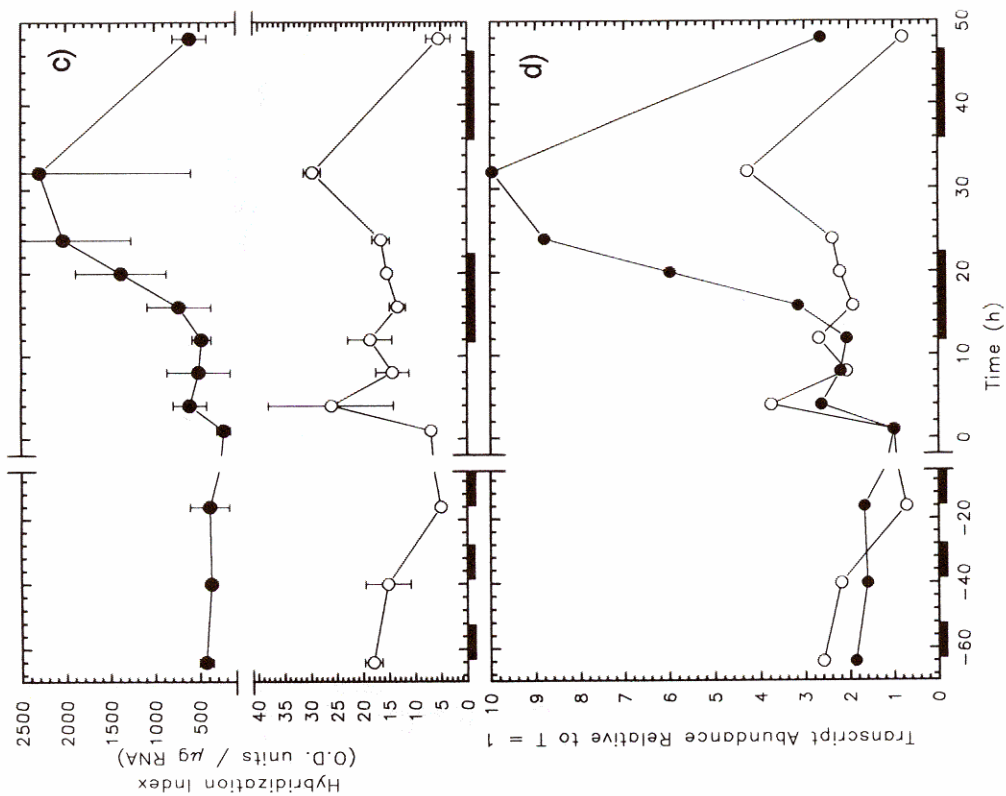
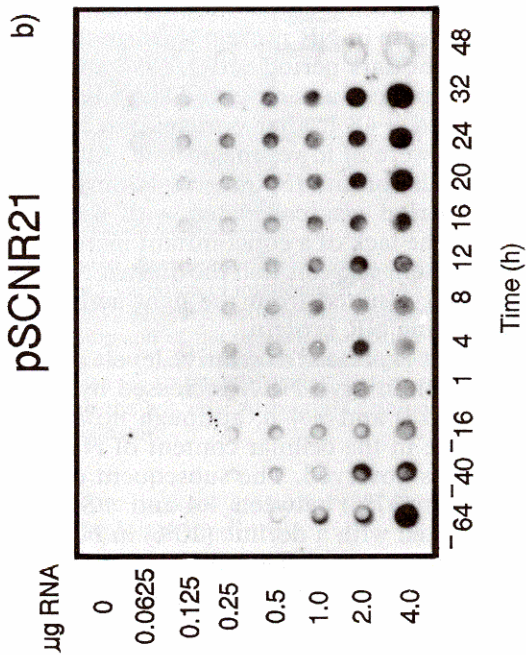
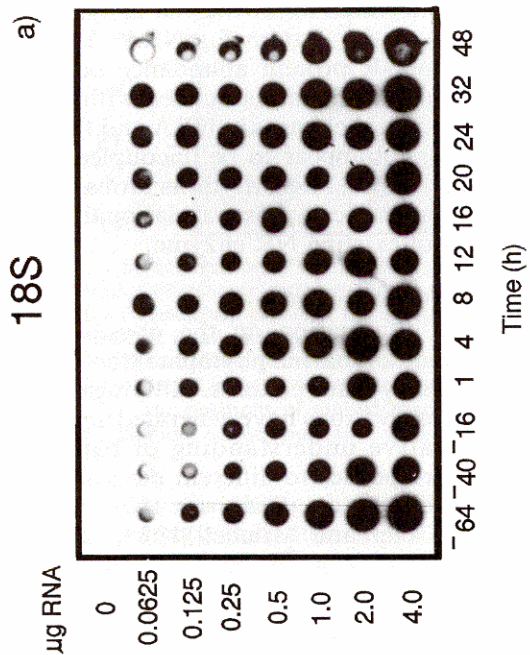


Fig. 7. Northern blot of *Skeletonema costatum* total RNA demonstrating specificity of the 18S ribosomal and NR cDNA probes and relative size of corresponding transcripts. Equal amounts of RNA (5 μg) were loaded and, after electrophoresis and transfer, the blot was hybridized sequentially with random-primed labeled *S. costatum* 18S rRNA probe and NR cDNA clone pSCNR21. Lane M—RNA ladder (BRL) with relative sizes indicated in kb; lane 1—ethidium bromide-stained gel of total RNA; lane 2—autoradiograph of northern blot using the 18S small subunit rRNA probe; lane 3—autoradiograph of northern blot using the NR cDNA (pSCNR21) probe.

content declined following cell division, in contrast to the pattern for NRA. The increase in NR protein abundance between +32 and +48 h was associated with a loss of NRA. Since changes in NRA and the NR protein pool appear to be uncoupled temporally, diurnal NRA rhythms probably reflect light-induced, posttranslational modulation of existing NR enzyme.

Discussion

Most information on the physiological adaptation of marine phytoplankton comes from steady state cultures. Although these static observations have generated a precise quantitative understanding of balanced growth responses to different environmental conditions (e.g. Bannister 1979; Shuter 1979; Kiefer and Mitchell 1983), the resulting theory explains little of the fine-scale temporal variability observed in the ocean (Cullen 1990). At least part of the problem may stem from the inability of steady state



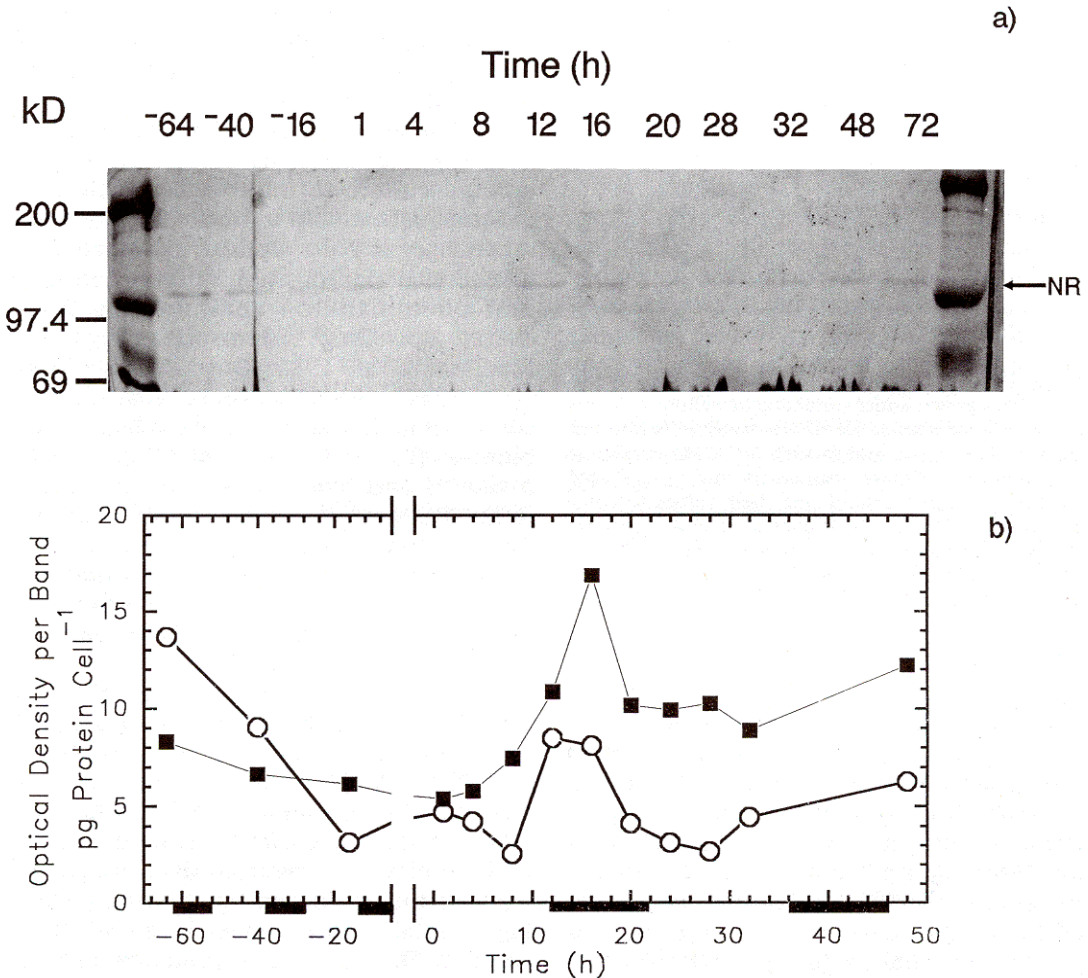


Fig. 9. Analysis of changes in abundance of NR protein in *Skeletonema costatum* cells during simulated upwelling. [a.] Western blot of total cellular protein profiles probed with antisera to squash NR and visualized with alkaline phosphatase-coupled secondary antibodies. Arrow indicates location of the polypeptide band cross-reacting with NR antisera. Equal amounts of protein (50 μ g) from sequential samples relative to the start of the enrichment were separated on a 7.5% SDS-PAGE and transferred to a nitrocellulose membrane. The position and size of mol-wt markers (kD) separated on the same gel are indicated on the left. [b.] Temporal variation in cellular protein content (■) (as in Fig. 6b) and the relative abundance of the NR cross-reactive protein (○) determined by densitometry of the alkaline phosphatase-positive bands shown in the top panel. Optical densities of each band were baseline corrected to the density background in each lane.

←

Fig. 8. Characterization of the abundance patterns of the small subunit rRNA (18S) and NR transcripts in total RNA isolated from *Skeletonema costatum* during simulated upwelling. [a, b.] Autoradiographs of dot blots of total RNA isolated from *S. costatum* during the simulated upwelling. Serial dilutions of glyoxal denatured RNA (4 μ g to 63 ng, rows) from each time point (columns) were applied to Nytran membranes and hybridized with the 18S rRNA probe (panel a) or the NR probe pSCNR21 (panel b). [c.] Quantification of changes in the abundance of 18S (●) and pSCNR21 (○) hybridizing sequences. Autoradiographs of hybridized dot blots were scanned with a densitometer and the change in exposure intensity (O.D.) with the weight of RNA per dot was determined by linear regression and expressed as the exposure slope. Error bars represent standard errors of the regression slopes. [d.] Changes in the abundance of the 18S rRNA (●) and pSCNR21 (○) transcripts relative to levels observed at the start of the light and NO_3^- enrichment (time = +1 h).

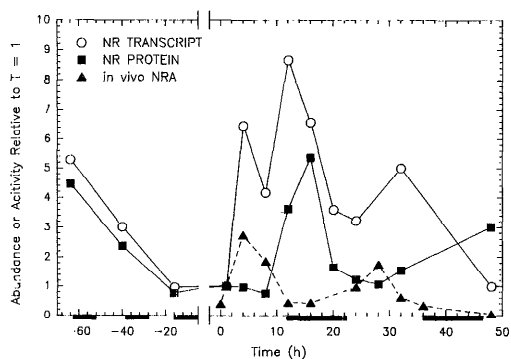


Fig. 10. Regulation of NRA in *Skeletonema costatum* cells grown under simulated upwelling. Changes in the cellular abundance of NR transcripts (O), NR (■) protein content, and in vivo NRA (▲) relative to the abundance of these components at $t = +1$ h after enrichment after standardizing their values to equal cell number. Trends show phasing of NR transcript and protein accumulation in response to light and NO_3^- enrichment. Initial increases in NRA occurred in the absence of appreciable NR enzyme accumulation, indicating light modulation of NRA rather than de novo synthesis.

theory to accommodate unbalanced growth resulting from temporal lags in metabolic responses to environmental shifts. These lags are exhibited by most unicellular organisms, including marine phytoplankton (Collos 1986), and presumably reflect interactions among different levels of cellular control (transcription, translation, and posttranslational modification) on the physiological pathways influenced by those environmental parameters.

Although the ecologically relevant time scales of adaptation pertain to natural, mixed-species phytoplankton assemblages, successional changes in species composition of the assemblage during a bloom event (Chavez et al. 1990; Pitcher 1990) may obscure the analysis of events controlling molecular and physiological processes sensitive to changing environments. In contrast, the experimental approach used here enabled precise observations of the physiological, biochemical, and molecular responses of N-stressed *S. costatum* cells to improved conditions of light and NO_3^- availability simulating a brief upwelling pulse. These laboratory observations indicate that induction of NO_3^- metabolism in response to environmental shifts is a cell-specific phe-

nomenon that reflects differential temporal responses of the molecular components regulating cellular energetics as well as assimilation of C and N.

Physiological responses to simulated upwelling—The transient responses of this unialgal culture to improved growth conditions qualitatively mimicked the temporal changes in NO_3^- uptake, C uptake, and biochemical composition observed in natural phytoplankton communities from coastal upwelling systems (Barlow 1982; MacIsaac et al. 1985; Dugdale and Wilkerson 1989), although events occurred on a compressed time scale due to the high initial biomass (2.3×10^6 cells ml^{-1} ; $700 \mu\text{g Chl } a$ liter $^{-1}$) and low relative N enrichment (DIN: PON = 0.43) used here. In contrast, freshly upwelled seawater is generally characterized by DIN: PON ratios > 1 and Chl *a* levels $< 1 \mu\text{g Chl } a$ liter $^{-1}$ (Wilkerson and Dugdale 1987; Dugdale and Wilkerson 1989). Prior to the light and NO_3^- enrichment, the cells were N deficient (C: N = 9.9) with respect to the Redfield ratio, and indices of NO_3^- assimilation capacity ($V^{15}\text{NO}_3$, $V\text{NRA}$) were low. The rates of induction or acceleration of $V^{15}\text{NO}_3$ and $V\text{NRA}$ following enrichment were comparable to observations from natural upwelling systems exhibiting lower absolute but higher relative enrichment levels (Wilkerson and Dugdale 1987). Increases in cell-specific $^{15}\text{NO}_3^-$ uptake and NRA were confined to the first light period when NO_3^- was present in the media, indicating that NO_3^- plays a direct role in metabolic induction. These observations also suggest that species-specific partitioning of NO_3^- (e.g. storage vs. growth; see Collos 1986) may influence the temporal pattern of induction of NO_3^- metabolism in natural systems.

The effect of improved growth conditions on photosynthetic performance was also dramatic. While rates of CO_2 fixation declined initially, rates of oxygenic photosynthesis increased, suggesting that the increased reducing power generated through enhanced photosynthetic electron transport was being used to drive the assimilation of NO_3^- at the expense of CO_2 fixation. The increase in photosynthetic efficiency (α) at +8 h also indicates a redirection of ab-

sorbed light energy toward NO_3^- reduction. The increase in NO_3^- assimilation capacity was also associated with a 3-fold increase in dark respiration, which could increase pools of reductant and (or) C skeletons for NO_3^- assimilation as has been hypothesized for green algae (Weger and Turpin 1989). Enhanced respiration during this period was also associated with an overall increase in energy-dependent anabolic processes such as nucleic acid and protein synthesis. Thus, although the relative NO_3^- enrichment used here was not sufficient to reverse the N-deficient status of the cells (based on C:N ratio), it did induce large and temporally significant transients in rates of photosynthesis and NO_3^- assimilation that can affect the biological dynamics of natural upwelling systems.

Regulation of NRA—The rate of induction of NO_3^- utilization capacity may control the rate of phytoplankton growth in N-limited environments characterized by a pulsed NO_3^- supply. The molecular aspects of NO_3^- assimilation, particularly the potentially rate-limiting activity of NR, have been well characterized in higher plants, but this information is lacking for phytoplankton (Campbell 1989; Solomonson and Barber 1990). NR expression is known to be influenced by light availability and source of N at the levels of gene transcription, RNA translation, and posttranslational modulation of enzyme activity. This study demonstrated that environmentally induced changes in NR transcript and protein abundance may underlie the adaptive response of phytoplankton to shifts in environmental conditions.

Rapid responses of phytoplankton cells to improved growth conditions may entail activation of existing enzyme pools as well as increased transcription and translation. Changes in the NRA of *S. costatum* cells observed here reflected both increased synthesis of enzyme and activity modulation of existing NR protein. The rapid increase in NR transcript abundance after the environmental shift also provides clear evidence that light and NO_3^- availability can induce NR gene expression in diatoms. Dependence of NR transcription on light and availability of N is further suggested by the

declines in NR transcript abundance during NH_4^+ -enriched and light-limited culture (−60 to 0 h) and during darkness (+12 to +22 h) since increases in NR transcript levels were restricted to periods of photosynthetically saturating PPF (see Fig. 10).

NR transcription and translation appeared to be coupled during the light-limited phase (−40 to 0 h) as NR transcript and protein abundance declined in parallel. These processes became uncoupled, however, after the shift to improved growth conditions, where the rapid increase in NR transcript and activity levels were not immediately associated with a concomitant increase in NR protein levels. In fact, at the cellular level, there was a general lag between the increase in transcript abundance and protein synthesis, presumably reflecting the time required to accumulate biochemical components required for protein synthesis.

NR protein may also be synthesized constitutively during the cell cycle of *S. costatum*, since the doubling in abundance of enzyme at +12 h after enrichment and subsequent reduction to pre-enrichment levels by +24 h was associated with the period of cell division. Accumulation of protein during the dark period is consistent with observations of oceanic phytoplankton in which sustained protein synthesis at night was attributed to the reapportionment of photosynthate (Cuhel et al. 1984).

In vivo NRA exhibited a pronounced diurnal rhythm that did not correspond to changes in NR protein levels, indicating that posttranslational modulation of enzyme activity may be light-dependent. Although in vitro NRA assays have been shown to track NR protein abundance in higher plant leaves and a green alga (Solomonson and Barber 1990; Velasco et al. 1989), our data demonstrate that diel changes in in vivo NRA reflect physiological levels of regulation independent of changes in enzyme abundance in *S. costatum*. The uncoupling of NRA and enzyme abundance, as well as the decline in NRA after NO_3^- depletion, demonstrates that both illumination and NO_3^- availability directly influence in vivo NRA. In addition, diurnal rhythms in NRA have been observed in marine phytoplankton com-

munities and macrophytic algae with both *in vitro* and *in vivo* assays (Martinez et al. 1987; Gao et al. 1992). Thus, caution must be taken to ensure that conclusions drawn regarding environmentally regulated induction of NRA in marine algae are not biased by underlying rhythms.

Under the experimental conditions used here, an absence of diurnal cycles in NO_3^- uptake and photosynthetic capacity of *S. costatum* cells indicates that diurnal modulation of NRA occurs independently of other changes in the physiological status of the cell and most likely reflects a direct role of light in the activation of existing NR protein. Accumulation of NR protein during the dark period after enrichment does suggest, however, that some increase in NR protein synthesis and (or) its stability resulted from the experimental treatment. Although the qualitative pattern is clear from this investigation, the quantitative effects of light and NO_3^- availability on induction of NO_3^- metabolism remain to be determined.

Biochemical markers of responses to transient conditions—A suite of biochemical parameters has been proposed to indicate nitrogen status in phytoplankton, providing information on prior sources of N and an index of growth potential for phytoplankton populations (Dortch and Postel 1989; Flynn 1990). If they are to serve as useful indices of cellular features, biochemical parameters should respond on time scales corresponding to the temporal patterns of environmental change. For example, RNA and protein content have been suggested as suitable markers for N status (Dortch et al. 1983; Dortch and Postel 1989) because, together, they account for upward of 80% of cellular N content (Wheeler 1983). Further, variation in the biochemical marker should be expressed on a cell-specific basis or under field conditions, normalized to a measure of biomass that varies directly with cell number.

In the present study, a very pronounced transient in cellular RNA content was observed that preceded changes in Chl *a*, protein, and DNA levels associated with the phased cell division (see Fig. 5), thus meeting the requirements outlined above. RNA : DNA ratios also provide a clear sig-

nal of rapid response to the improved growth conditions in the present study. This ratio returned to baseline levels after a round of cell division and in response to N depletion. Interestingly, the baseline RNA : DNA ratio (wt basis) was similar for both the light- and N-limited phases of the treatment, supporting previous observations that this ratio is a useful marker for transient improvements in phytoplankton growth conditions and metabolic status (Dortch et al. 1983).

Application of standard molecular biology techniques provided sensitive markers of the molecular mechanisms associated with the response of phytoplankton cells to variable environments. Underlying the transient increase in the RNA content of *S. costatum* after enrichment was a rhythmic variation in the translational capacity that was synchronized with the light phase of the photoperiod. Previous studies of green algae and higher plants have documented light-dependent transcription of some nuclear- and chloroplast-encoded genes (Puisseux-Dao 1981; Tobin and Silverthorne 1985). In this study the initial peak in translational capacity was associated with the period of maximal protein accumulation. The second peak in translational capacity, however, occurred after the onset of NO_3^- depletion from the medium and was not associated with any net accumulation of protein, suggesting that NO_3^- depletion inhibited some components of the translational machinery (e.g. amino acid availability). Sensitive measures of the uncoupling between the availability of mRNAs (translational capacity) and realized rates of protein synthesis may elucidate key metabolic steps that dictate lags in phytoplankton growth in response to environmental shifts.

The dynamics of RNA transcript populations can be dissected further through hybridization analyses with specific gene probes. In the present study, the small-subunit rRNA and NR transcripts exhibited different behaviors. Levels of both transcripts increased in the initial response to improved light and NO_3^- conditions for growth and again during the second photoperiod, after NO_3^- had been depleted from the medium, suggesting that transcript accumulation may respond to internal rather

than external levels of N, as has been observed previously for NRA in *S. costatum* (Dortch 1982). The abundance of 18S rRNA tracked the translational capacity of the total RNA more closely than did the abundance of NR transcripts. The dynamics of 18S rRNA, with its primary role in protein synthesis, in addition to ease of detection due to its high abundance in the cell, suggest that 18S rRNA abundance may be a useful index of the growth potential of phytoplankton cells, as has been demonstrated for bacteria (DeLong et al. 1989).

The dynamics of specific RNA transcripts can also be sensitive indicators of changes in the metabolic status of phytoplankton cells and may serve as reliable markers of shifts in specific metabolic pathways in response to environmental transients. This approach has real promise for oceanographic applications since bulk measures of RNA and DNA content can be performed routinely on oceanic water samples (Dortch et al. 1983), and nucleic acids of suitable quality for molecular analysis can be obtained with only minor modifications of existing protocols (Giovannoni et al. 1990; G. J. Smith unpubl. data). Northern analysis with taxon-specific gene probes can be used to track functional markers of individual taxa among heterogeneous mixtures of RNAs obtained from natural oceanic samples, as used to examine bacterial diversity in natural systems (Giovannoni et al. 1990).

Environmental regulation of critical metabolic processes, such as NO_3^- assimilation, can be assessed at the molecular level by simultaneously monitoring the abundance of specific transcripts, proteins, and enzyme activities in oceanic samples as reported here for laboratory-grown phytoplankton. Application of these techniques in oceanic environments in conjunction with measurements of water-column biological and physical characteristics are essential for development of a mechanistic understanding of the influence of metabolic lags on temporal and spatial dynamics of phytoplankton bloom formation. Such knowledge is critical to the development of quantitative models that can accommodate the nonlinearity of biological phenomena and yield new insights into oceanic processes.

This laboratory study, based on the concurrent monitoring of whole-cell physiological and subcellular molecular events associated with the transition of light-limited and N-deficient *S. costatum* cells to light and NO_3^- enrichment, has demonstrated that the cellular changes observed here are qualitatively similar to the responses of natural phytoplankton assemblages to improved growth conditions characteristic of coastal upwelling systems. Furthermore, the physiological and molecular responses described here can provide a partial, mechanistic explanation for performance shifts observed in field populations. Cellular lags in responses to environmental transients can be related to an uncoupling of C and N assimilation and the feedback of these physiological features on the molecular processes that govern their expression. It is anticipated that further investigations into the cellular and molecular processes that govern N and C assimilation will not only improve understanding of growth dynamics of marine phytoplankton but advance the ability to predict temporal and spatial patterns of oceanic primary production.

References

- APARICIO, P. J., J. M. ROLDAN, AND F. CALERO. 1976. Blue light photoreactivation of nitrate reductase from green algae and higher plants. *Biochem. Biophys. Res. Comm.* **70**: 1071-1077.
- BANNISTER, T. T. 1979. Quantitative description of steady state nutrient-saturated algal growth, including adaptation. *Limnol. Oceanogr.* **24**: 76-96.
- BARLOW, R. G. 1982. Phytoplankton ecology in the southern Benguela Current. 3. Dynamics of a bloom. *J. Exp. Mar. Biol. Ecol.* **63**: 239-248.
- BEEVERS, L., AND R. H. HAGEMAN. 1980. Nitrate and nitrite reduction, p. 115-168. *In* P. K. Stumpf et al. [eds.], *The biochemistry of plants. A comprehensive treatise*. V. 5. Academic.
- BONNER, W. M., AND R. A. LASKEY. 1974. A film detection method for tritium labeled proteins and nucleic acids in polyacrylamide gels. *Eur. J. Biochem.* **46**: 83-88.
- BRUNETTI, N., AND R. H. HAGEMAN. 1976. Comparison of in vivo and in vitro assays of nitrate reductase in wheat (*Triticum aestivum* L.) seedlings. *Plant Physiol.* **58**: 583-587.
- CAMPBELL, W. H. 1989. Structure and regulation of nitrate reductase in higher plants, p. 125-154. *In* J. L. Wray and J. R. Kinghorn [eds.], *Molecular and genetic aspects of nitrate assimilation*. Oxford.
- CHAVEZ, F. P., K. R. BUCK, AND R. T. BARBER. 1990. Phytoplankton taxa in relation to primary pro-

- duction in the equatorial Pacific. *Deep-Sea Res.* **37**: 1733-1752.
- CHOMCZYNSKI, P., AND N. SACCHI. 1987. Single-step method of RNA isolation by acid guanidinium thiocyanate-phenol-chloroform extraction. *Anal. Biochem.* **162**: 156-159.
- CODISPOTI, L. A. 1983. Nitrogen in upwelling systems, p. 513-564. *In* E. J. Carpenter and D. G. Capone [eds.], *Nitrogen in the marine environment*. Academic.
- , R. C. DUGDALE, AND J. H. MINAS. 1982. A comparison of nutrient regimes off northwest Africa, Peru and Baja California. *J. Cons. Cons. Int. Explor. Mer* **180**: 184-201.
- COLLOS, Y. 1982. Transient situations in nitrate assimilation by marine diatoms. 3. Short-term uncoupling of nitrate uptake and reduction. *J. Exp. Mar. Biol. Ecol.* **62**: 285-295.
- . 1986. Time-lag algal growth dynamics: Biological constraints on primary productivity in aquatic environments. *Mar. Ecol. Prog. Ser.* **33**: 193-206.
- COVE, D. J., AND J. A. PATEMAN. 1969. Autoregulation of the synthesis of nitrate reductase in *Aspergillus nidulans*. *J. Bacteriol.* **97**: 1374-1378.
- CUHEL, R. L., P. B. ORTNER, AND D. R. S. LEAN. 1984. Night synthesis of protein by algae. *Limnol. Oceanogr.* **29**: 731-744.
- CULLEN, J. J. 1990. On models of growth and photosynthesis in phytoplankton. *Deep-Sea Res.* **37**: 667-683.
- DELONG, E. F., G. S. WICKHAM, AND N. R. PACE. 1989. Phylogenetic stains: Ribosomal RNA-based probes for the identification of single cells. *Science* **243**: 1360-1363.
- DORTCH, Q. 1982. Effect of growth conditions on accumulation of internal nitrate, ammonium, amino acids and protein in three marine diatoms. *J. Exp. Mar. Biol. Ecol.* **61**: 243-264.
- , AND J. R. POSTEL. 1989. Biochemical indicators of N utilization by phytoplankton during upwelling off the Washington coast. *Limnol. Oceanogr.* **34**: 758-773.
- , T. L. ROBERTS, J. R. CLAYTON, JR., AND S. I. AHMED. 1983. RNA/DNA ratios and DNA concentrations as indicators of growth rate and biomass in planktonic marine organisms. *Mar. Ecol. Prog. Ser.* **13**: 61-71.
- DUGDALE, R. C., AND J. J. GOERING. 1967. Uptake of new and regenerated forms of nitrogen in primary productivity. *Limnol. Oceanogr.* **12**: 196-206.
- , AND F. P. WILKERSON. 1986. The use of ^{15}N to measure nitrogen uptake in eutrophic oceans; experimental considerations. *Limnol. Oceanogr.* **31**: 673-689.
- , AND ———. 1989. New production in the upwelling center at Point Conception, California: Temporal and spatial patterns. *Deep-Sea Res.* **36**: 985-1007.
- , ———, AND A. MOREL. 1990. Realization of new production in coastal upwelling areas: A means to compare relative performance. *Limnol. Oceanogr.* **35**: 822-829.
- FEINBERG, A. P., AND B. VOLGELSTEIN. 1983. A technique for radiolabeling DNA restriction endonuclease fragments to high specific activity. *Anal. Biochem.* **132**: 6-13.
- FLYNN, K. J. 1990. The determination of nitrogen status in microalgae. *Mar. Ecol. Prog. Ser.* **61**: 297-307.
- GAO, Y., G. J. SMITH, AND R. S. ALBERTE. 1992. Light regulation of nitrate reductase in *Ulva fenestrata* (Chlorophyceae). I. Influence of light regimes on nitrate reductase activity. *Mar. Biol.* **112**: 691-696.
- GARSDALE, C. 1991. Shift-up and the nitrate kinetics of phytoplankton in upwelling systems. *Limnol. Oceanogr.* **36**: 1239-1244.
- GIOVANNONI, S. J., T. B. BRITSCHEG, C. L. MOYER, AND K. G. FIELD. 1990. Genetic diversity in Sargasso Sea bacterioplankton. *Nature* **345**: 60-63.
- GUILLARD, R. R. L. 1975. Culture of phytoplankton for feeding marine invertebrates, p. 29-60. *In* W. L. Smith and M. H. Chanley [eds.], *Culture of marine invertebrate animals*. Plenum.
- HIPKIN, C. R., AND P. J. SYRETT. 1977. Post-transcriptional control of nitrate reductase formation in green algae. *J. Exp. Bot.* **28**: 1270-1277.
- INGRAHAM, J. L., O. MAALOE, AND F. C. NEIDHARDT. 1983. Growth of the bacterial cell. Sinauer.
- JEFFREY, S. W., AND G. F. HUMPHREY. 1975. New spectrophotometric equations for determining chlorophylls *a*, *b*, *c*₁ and *c*₂ in higher plants, algae and natural phytoplankton. *Biochem. Physiol. Pflanz.* **167**: 191-194.
- KIEFER, D. A., AND B. G. MITCHELL. 1983. A simple, steady state description of phytoplankton growth based on absorption cross section and quantum efficiency. *Limnol. Oceanogr.* **28**: 770-776.
- LAEMMLI, U. K. 1970. Cleavage of structural proteins during the assembly of the head of bacteriophage T4. *Nature* **227**: 680-685.
- MACISAAC, J. J., R. C. DUGDALE, R. T. BARBER, D. BLASCO, AND T. T. PACKARD. 1985. Primary production cycle in an upwelling center. *Deep-Sea Res.* **32**: 503-529.
- MANIATIS, T., E. F. FRITSCH, AND J. SAMBROOK. 1982. *Molecular cloning—a laboratory manual*. Cold Spring Harbor Lab.
- MARTINEZ, R., T. T. PACKARD, AND D. BLASCO. 1987. Light effects and diel variations of nitrate reductase activity in phytoplankton from the northwest Africa upwelling region. *Deep-Sea Res.* **34**: 741-753.
- PACKARD, T. T. 1973. The light dependence of nitrate reductase in marine phytoplankton. *Limnol. Oceanogr.* **18**: 466-469.
- PITCHER, G. C. 1990. Phytoplankton seed populations of the Cape Peninsula upwelling plume, with particular reference to resting spores of *Chaetoceros* (Bacillariophyceae) and their role in seeding upwelling waters. *Estuarine Coastal Shelf Sci.* **31**: 283-301.
- PLUMLEY, F. G., AND G. W. SCHMIDT. 1989. Nitrogen-dependent regulation of photosynthetic gene expression. *Proc. Natl. Acad. Sci.* **86**: 2678-2682.
- PUISEUX-DAO, S. 1981. Cell-cycle events in unicellular algae, p. 130-149. *In* *Can. Bull. Fish. Aquat. Sci.* **210**.

- REDINBAUGH, M. G., AND W. H. CAMPBELL. 1983. Purification of squash NADH: nitrate reductase by zinc chelate affinity chromatography. *Plant Physiol.* **71**: 205–207.
- SAIKI, R. K., AND OTHERS. 1988. Primer-directed enzymatic amplification with a thermostable DNA polymerase. *Science* **239**: 487–491.
- SAKSHAUG, E., AND O. HOLM-HANSEN. 1977. Chemical composition of *Skeletonema costatum* (Grev.) Cleve and *Pavlova (Monochrysis) lutheri* (Droop) Green as a function of nitrate-, phosphate- and iron-limited growth. *J. Exp. Mar. Biol. Ecol.* **29**: 1–34.
- SCHAECTER, M. 1968. Growth: Cells and populations, p. 136–162. *In* T. Mandelstam and K. McQuillen [eds.], *Biochemistry and bacterial cell growth*. Wiley-Interscience.
- SHUTER, B. 1979. A model of physiological adaptation in unicellular algae. *J. Theor. Biol.* **78**: 519–522.
- SMITH, P. K., AND OTHERS. 1985. Measurement of protein using bicinchoninic acid. *Anal. Biochem.* **150**: 76–85.
- SOGIN, M. L. 1990. Amplification of ribosomal RNA genes for molecular evolution studies, p. 307–314. *In* M. A. Innis et al. [eds.], *PCR protocols: A guide to methods and applications*. Academic.
- SOLOMONSON, L. P., AND M. J. BARBER. 1990. Assimilatory nitrate reductase: Functional properties and regulation. *Annu. Rev. Plant Physiol. Plant Mol. Biol.* **41**: 225–253.
- STRICKLAND, J. D. H., AND T. R. PARSONS. 1972. *A practical handbook of seawater analysis*, 2nd ed. *Bull. Fish. Res. Bd. Can.* **167**.
- THOMAS, P. S. 1983. Hybridization of denatured RNA transferred or dotted to nitrocellulose paper. *Methods Enzymol.* **100**: 255–266.
- TOBIN, E. M., AND J. SILVERTHORNE. 1985. Light regulation of gene expression in higher plants. *Annu. Rev. Plant Physiol.* **36**: 569–593.
- TOWBIN, H., AND J. GORDON. 1984. Immunoblotting and dot immunoblotting—current status and outlook. *J. Immunol. Methods* **72**: 313–340.
- VELASCO, P. J., R. TISCHNER, R. C. HUFFAKER, AND J. R. WHITAKER. 1989. Synthesis and degradation of nitrate reductase during the cell cycle of *Chlorella sorokiniana*. *Plant Physiol.* **89**: 220–224.
- WAHL, G. M., J. L. MEINKOTH, AND A. R. KIMMEL. 1987. Northern and southern blots. *Methods Enzymol.* **152**: 572–581.
- WEGER, H. G., AND D. H. TURPIN. 1989. Mitochondrial respiration can support NO_3^- and NO_2^- reduction during photosynthesis. Interactions between photosynthesis, respiration, and N assimilation in the N-limited green alga *Selenastrium minutum*. *Plant Physiol.* **89**: 409–415.
- WHEELER, P. A. 1983. Phytoplankton nitrogen metabolism, p. 309–346. *In* E. J. Carpenter and D. G. Capone [eds.], *Nitrogen in the marine environment*. Academic.
- WILKERSON, F. P., AND R. C. DUGDALE. 1987. The use of large shipboard barrels and drifters to study the effects of coastal upwelling on phytoplankton dynamics. *Limnol. Oceanogr.* **32**: 368–382.
- ZIMMERMAN, R. C., J. N. KREMER, AND R. C. DUGDALE. 1987. Acceleration of nutrient uptake by phytoplankton in a coastal upwelling ecosystem: A modeling analysis. *Limnol. Oceanogr.* **32**: 359–367.

Submitted: 30 July 1991

Accepted: 2 December 1991

Revised: 13 March 1992